atmosphere

MDPI

Article

Behavior of Selenium during Chemical-Looping Gasification of Coal Using Copper-Based Oxygen Carrier

Jingjing Ma *,†, Jiameng Hu †, Huifen Kang, Ziheng Han and Qingjie Guo *

State Key Laboratory of High-Efficiency Utilization of Coal and Green Chemical Engineering, Ningxia University, Yinchuan 750021, China; hu_jmeng@163.com (J.H.); huifen_kang@163.com (H.K.); hanziheng0531@163.com (Z.H.)

* Correspondence: majingjing@nxu.edu.cn (J.M.); qingjie_guo@nxu.edu.cn (Q.G.); Tel./Fax: +86-951-2062323 (J.M. & Q.G.)

† These authors contributed equally to this work.

Abstract: The migration and transformation behavior of selenium during coal chemical looping gasification (CLG) under the impact of a CuO/Bentonite (Ben) oxygen carrier (OC) were studied in a batch fluidized bed reactor. In the CLG process, the total percentage of selenium released in gaseous phase was 73.06%. In the conventional gasification process, 91.71% of the total selenium was released in a gaseous state. The addition of CuO/Ben OC apparently promoted the transformation from gaseous selenium to particulate selenium. The oxygen–carbon ratio (O/C) played an important role in affecting the fraction of gaseous selenium released in the gasification process, with results showing that the amount of selenium adsorbed by CuO/Ben OC was added along with the increase in OC. By means of X-ray photoelectron spectroscopy (XPS) characterization, we found that the reduced CuO/Ben OC contained a small amount of Cu_2Se due to the oxidation and adsorption of selenium onto their porous surface. The regeneration performance of the CuO/Ben OC was favorable after 10 regeneration cycles of the CLG process. The increase in the pore volumes and specific surface areas contributed to the enhanced capacity of retaining selenium for CuO/Ben OC.

Keywords: selenium; chemical-looping gasification; CuO/bentonite oxygen carrier; transformation mechanism; migration

Citation: Ma, J.; Hu, J.; Kang, H.; Han, Z.; Guo, Q. Behavior of Selenium during Chemical-Looping Gasification of Coal Using Copper-Based Oxygen Carrier. *Atmosphere* **2022**, *13*, 547. https://doi.org/10.3390/atmos13040547

Academic Editor: Jaroslaw Krzywanski

Received: 28 February 2022
Accepted: 23 March 2022
Published: 29 March 2022

1. Introduction

Chemical looping gasification (CLG) has great potential in the use of solid fuels [1–3]. For the production and utilization of syngas, CLG technology has the advantages of being highly efficient and clean, and the transfer of heat and oxygen is realized by using an oxygen carrier (OC) between the fuel reactor (FR) and air reactor (AR). Compared with conventional gasification technology, CLG technology can effectively control synthesis gas, reduce oxygen consumption and control NOx production [4–7].

Selenium is a highly volatile trace element in coal, and also a potentially toxic microelement in coal. Different forms of selenium will be released from coal-burning factories through coal gasification and combustion, and will mainly be distributed in the gas phase [8], which will discharge the gaseous selenium into the atmosphere and endanger human life if it is not mitigated in a timely manner [9–11]. Exposure to high concentrations of gaseous selenium for less than a minute can lead to acute poisoning and at least several days of experiencing cold symptoms [12]. Generally, selenium can effectively be removed by various absorbent materials or catalysts [13–15]. The discoveries about the behavior of selenium during coal gasification and combustion have been extensively reported [8,16,17], which can be used for reference to some extent. Shen et al. [18] found the content of gaseous selenium released by the coal gasification process was higher than the coal combustion process. The morphology and chemical characteristics of selenium on the ash surface were detected by Fu et al. [19]. The results show that the elemental selenium was predominantly higher in abundance. However, because of the transfer of lattice oxygen and active sites

on OCs surface, the behaviors of selenium may be very different from that of CLG. The environmentally-unfriendly and poisonous trace elements (TEs), such as Hg and Se in coal, can migrate and transform in a chemical looping process [20–22]. The form of selenium occurring in coal, and the different coal types, are important factors affecting its migration and transformation [23,24]. Despite all this, the behavior of selenium in CLG has not yet been discovered, with research on contaminants in chemical-looping processes focusing instead on phosphorus, mercury, cadmium and sulfur [25–29]. Therefore, research on the migration and transformation of selenium in the presence of OC is innovative and enlightening. It is essential to discover the migration and transformation mechanism of selenium in CLG, with the aim of developing effective control methods.

OC serves as a key medium in CLG. The addition of OC is of particular importance for selenium distribution in coal ash, OC and flue gas. The separation of OC and coal ash after reaction is a prerequisite to the proposed migration mechanism in this study [30]. Among the various OCs, the copper-based OC is considered to be a suitable choice in CLG because of its strong oxygen transport capacity and high reactivity [31–34]. Al_2O_3, TiO_2, SiO_2 and bentonite are usually used as support materials. By contrast, the OC particles prepared with bentonite have large mechanical strength and improved wear resistance [35], which are more conducive to the bed materials separation by sieving and the recycling of OC.

The purpose of the project is to systematically discover the migration behavior of selenium during CLG and the possible partitioning from gaseous selenium to particulate selenium. Different bituminous coals and CuO Ben (Bentonite) OC were used as raw materials. The distribution of selenium in the CLG process was researched in a batch fluidized bed. In addition, the impacts of different fuels and oxygen-carbon ratios (O/C) on the migration of selenium between flue gas, OC and coal ash were also studied. The mechanism of selenium migration and transformation in CLG was proposed, which provided a theoretical basis for the effective control of selenium.

2. Experimental

2.1. Coal Samples and Oxygen Carriers

Three kinds of bituminous coals from Shaanxi (SX), Inner Mongolia (NM) and Ningxia (NX) were selected as fuels. The particle size of coal samples was divided into 80–100 mesh. The concentration of selenium in the above three kinds of coal can reach the detection limit. Table 1 included the composition analyses of the fuels and selenium concentration. Selenium content in coal is detected by an Atomic Fluorescence Spectrophotometer (AFS-993, Chian, Bjingjing, Jitian, the detection limit of selenium is 0.01 ug/L) and the ultimate of the coal is detected by element analyzer (EA300, Italy, Pavia, Euro Vector, the detection limit is 0.01 mg/g). The coal ash component of the fuel samples was listed in Table 2. Analysis of coal ash composition was undertaken by X-ray Fluorescence Spectrometry (PANalytical Axios, Netherlands, PANalytical B.V., the detection limit is 1 ppm).

Table 1. The ultimate and proximate analyses of the coal sample.

Sample	Proximate Analysis w_t/%				Ultimate Analysis w_t/%					
	M_{ad}	A_{ad}	V_{ad}	FC_{ad}	C_{ad}	H_{ad}	N_{ad}	S_{ad}	O_{ad}	Se(μg/g)
SX	7.14	5.84	29.71	57.31	69.08	7.17	0.76	0.3	14.03	0.36
NX	5.18	4.56	26.95	63.31	77.6	5.16	1.46	0.46	10.77	0.19
NM	11.52	5.07	27.26	56.15	74.08	4.91	0.7	0.02	14.29	0.17

Note: ad: air dried basis.

Table 2. Inorganic constituents of the coal sample.

Sample	SiO_2	Al_2O_3	Fe_2O_3	CaO	MgO	K_2O	Na_2O
SX ash	51.43	11.73	22.09	8.91	5.03	2.35	0.44
NX ash	47.87	13.62	18.86	7.19	7.73	2.84	0.55
NM ash	62.86	8.16	20.96	9.00	7.12	0.97	0.15

As part of this study, CuO/Ben (60:40 wt%) OC was prepared, to investigate how it affects the behavior of selenium. Bentonite was selected as the inert carrier for the CuO based OC, and was prepared by a mechanical stirring method. The produced CuO/Ben OC was screened into 30–50 mesh for subsequent experiments. The preparation process enhanced the mechanical strength of CuO/Ben OC, which was conducive to the separation of coal ash and OC after the gasification reaction. This is a premise to obtain the distribution of selenium in coal ash and OC.

2.2. Experimental Conditions and Methods

The experiments were conducted in a batch fluidized bed reactor. The equipment diagram was shown in Figure 1, the reaction system included a fluidized bed reactor, a flue gas analyzer and a steam generator. The tube was about 1000 mm and the inside diameter was 60 mm. Water steam was heated from the steam generator to 250 °C as the gasification agent after it had been produced by a controlled pump. The gasifying agent was carried by nitrogen into the reaction system from the bottom. Afterwards, the fuel gas was transported to the impingers that were prepared to absorb the gaseous selenium. A fuel gas analyzer was connected to detect the concentration of the coal gas products (CO, H_2, CH_4, N_2, and CO_2).

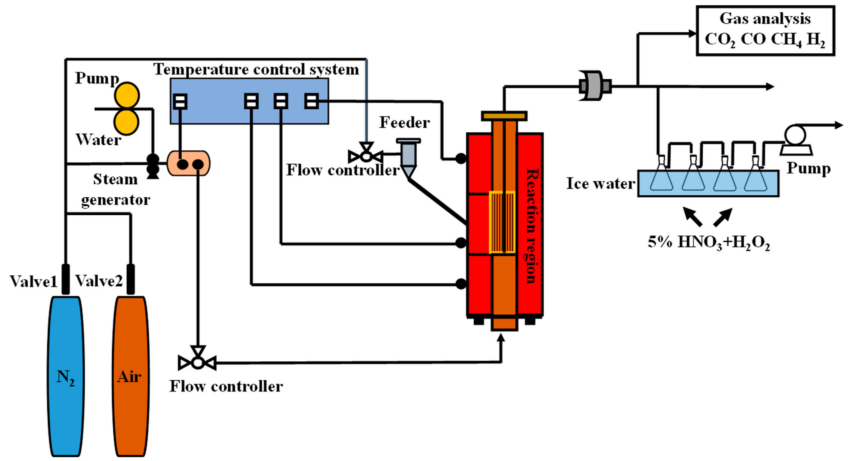

Figure 1. Schematic diagram of the laboratory setup.

All subsequent experiments were performed at an appropriate temperature of 900 °C. The amount of each experiment fuel sample was 3.0 g. According to the capacity of CuO/Ben OC to transport oxygen, the mass of CuO/Ben OC was calculated according to the O/C ratio of 0.4. The reaction agents were 50 vol% water vapor (1.1 g/min) in N_2 (the minimum fluidizing velocity (Umf) was 0.03 m/s, and the superficial gas velocity (U0) was 1.16 times Umf.) in the experiments. The above experimental conditions were derived from the preliminary research results of our team. The reaction time of all experiments was controlled at 60 min, which ensured that the above reactions could be fully completed. Silica was utilized as a bed material for the comparative experiment. Moving forward, experiments with different O/C ratios and different coal types were conducted to discover the behavior of selenium during CLG.

On account of the experiment being an intermittent operation, the CuO/Ben particles were utilized to complete the reduction and oxidation process, achieving a circulation process of chemical looping. For continuous circulation tests of CLG, air was forced into the fluidized bed chamber to regenerate OCs particles after each reduction reaction.

2.3. Analysis of Selenium

Due to the amount of selenium being very small, the precision of the selenium detection was of great importance to our work. An authoritative regulation for the sampling and measurement of gaseous selenium was adopted (ISO 17211:2015) [36]. After each batch of experiments was finished, the residues (coal ash for gasification, oxygen carriers and coal ash for CLG) were collected as solid samples, and the gaseous samples were derived from the impingers. A microwave processor (Multiwave PRO, Austria, Anton Paar) was employed to digest the solid materials following the standard procedures. The content of selenium after digestion was determined using an atomic fluorescence spectrophotometer (AFS-993, Beijing Jitian, and the detection limit of selenium is 0.01 ug/L). Moreover, the selenium contents on the fresh CuO/Ben oxygen carriers were also analyzed using the above measurement methods. The results showed that fresh oxygen carriers contained almost no selenium, and they could be neglected. Based on the standard issued by China: GB/T 16415-2008, it is stipulated that accurate detection results can be obtained by using AFS for selenium measurement. When the selenium content in coal is less than 6 ug/g, the repeatability limit can reach 1 ug/g. Therefore, AFS-993 can get accurate measurement results.

In order to ensure the reliability and accuracy of the results, the final experimental result is determined from the mean of the five parallel experiments. What needs illustration is that, due to some inevitable causes of error in the operation process and detection analysis, there are inevitable errors in the total selenium mass balance. In this research, the mass balance of selenium was between 87.60% and 100.39%, which means the final results are precise and convincing.

2.4. Thermodynamic Simulation

To guarantee the accuracy and reliability of the test result, the final experimental results were determined from the variance in the five parallel experiments. What needs illustration is that due to some inescapable errors in the operation process and detection analysis, there were inevitable errors in the total selenium mass balance. In this research, the mass balance of selenium was between 87.60% and 100.39%, which means the final results are precise and convincing [11].

2.5. Data Calculation

2.5.1. Selenium Mass Balance

The distribution coefficient *(DC)* is defined to partition the allocation of selenium, as follows:

$$DC = \frac{M_i}{M_{OC} + M_{FG} + M_{CA}} \times 100\% \quad (1)$$

where M_{OC} represents the absolute selenium mass of the CuO/Ben oxygen carriers, M_{FG} represents the absolute gaseous selenium from the absorption liquid, and M_{CA} represents the absolute selenium mass in the coal ash. i = (OC, FG, CA) and OC, FG, CA denote oxygen carrier, flue gas and coal ash, respectively.

The selenium recovery rate (*RR*) in the coal ash, flue gas and oxygen carriers is listed by:

$$RRi = \frac{M_i}{M_T} \times 100\% \quad (2)$$

where M_T denotes the whole mass of selenium.

2.5.2. The Indexes of CLG Performance

On a dry basis, the overall volume flow rate F_{out}, red is calculated through the nitrogen equilibrium, and the formula is as follows:

$$F_{out,red} = \frac{F_{in,N_2}}{1 - x_{CO} - x_{CO_2} - x_{CH_4} - x_{H_2} - x_{O_2}} \quad (3)$$

where F_{in} is the N_2 inlet volume flow rate, L/min and x_i are the instantaneous volume fractions of outlet gas (CO_2, CO, CH_4, H_2 and O_2), vol%.

In the dry base state, the volume flow rate of each outlet flue gas is defined as follows:

$$Y_i = \frac{\int_0^t F_{out,red} x_i dt}{\int_0^t F_{out,red}(x_{CO_2} + x_{CO} + x_{CH_4} + x_{H_2})dt} \quad (4)$$

where x_i (i = CO_2, CO, CH_4, H_2) represents the volume fraction of the outlet flue gas.

The synthetic gas yield (G_{syn}, Nm^3/kg) is calculated through the volume of outlet gas (CO, CH_4 and H_2) products generated on a dry basis by the following formula:

$$G_{syn} = \frac{\int_0^t F_{out,red}(x_{CO} + x_{CH_4} + x_{H_2})dt}{\int_0^t F_{out,red}(x_{CO_2} + x_{CO} + x_{CH_4} + x_{H_2})dt} \quad (5)$$

3. Results and Discussion

3.1. Gasification Characteristics

The CLG experiment was conducted at 900 °C, and the O/C ratio was 0.4, SX bituminous coal and CuO/Ben OCs were used as raw materials. Figure 2 compared the variation in volume gas flow rate with time during traditional gasification and CLG.

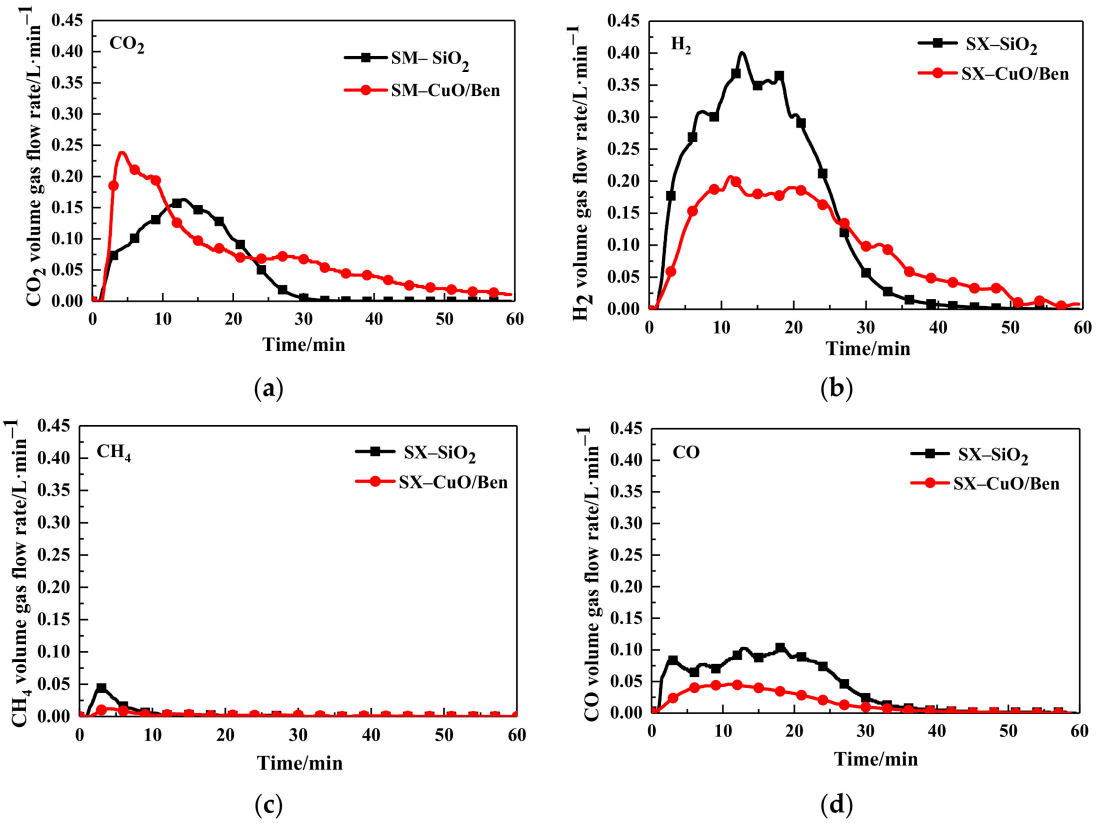

Figure 2. Gas concentration of (**a**) CO_2, (**b**) H_2, (**c**) CH_4, (**d**) CO, and using SX bitumite for quartz sand and CuO/Ben oxygen carriers.

The results showed that the trend in flue gas concentration curve increased first and then decreased with the addition of the reaction time for either process between SX bituminous coal and CuO/Ben OCs, or between SX bituminous coal and quartz sand (SiO_2), as shown in Figure 2a–d. The analyses of these charts showed that the concentration of CO_2 in CuO/Ben OC was significantly higher than that of SiO_2. The explanation was that CuO/Ben OCs reacted with syngas (CO, CH_4, H_2) to rapidly generate CO_2 and H_2O.

Table 3 lists the content of outlet gas and syngas yields during conventional gasification and CLG. Compared with coal gasification, the generation of CO, CH_4 and H_2 was reduced in the CLG process, which consumed part of the syngas to provide heat for the gasification reaction.

Table 3. The content of outlet gas and syngas yields of coal gasification and CLG.

Sample	Y_i (%)				G_{syn} (%)
	CO_2	CO	H_2	CH_4	
SX/SiO_2	20.85	18.02	59.44	1.69	0.82
SX/(CuO/Ben)	39.39	8.62	51.01	0.98	0.61

3.2. Morphology of Selenium in CLG

3.2.1. Selenium Distribution

Primarily, the distribution of selenium during traditional gasification and the CLG of SX bituminous coal was investigated. As shown in Figure 3, in the conventional gasification of silica sand as the bed material, the distribution of selenium in the coal ash and gaseous phase accounted for 8.29% and 91.71%, respectively. The proportion of gaseous selenium was larger, and that of the bed material only occupied a small part. The conclusion was similar to previous results. The selenium content in fly ash was not considered, due to the small production of fly ash. Compared with the traditional gasification process, the process of CLG involves a large amount of metal oxides that can oxidize and adsorb selenium. Thus, a peculiar effect on the distribution of selenium may appear in this form of gasification. Figure 3 showed that the content of H_2Se (g) decreased from 91.71% (with silica sand) to 73.65% (in CuO/Ben OC). Meanwhile, the content of selenium in OCs accounted for 19.07%, which showed that the addition of OCs could inhibit the volatilization of selenium in coal and a small amount of selenium migrated to OCs. Theoretically, the oxidation and adsorption of selenium by inorganic oxides in coal ash and unburned carbon were the main reasons to retain gaseous selenium. More selenium was successfully transformed into particulate selenium.

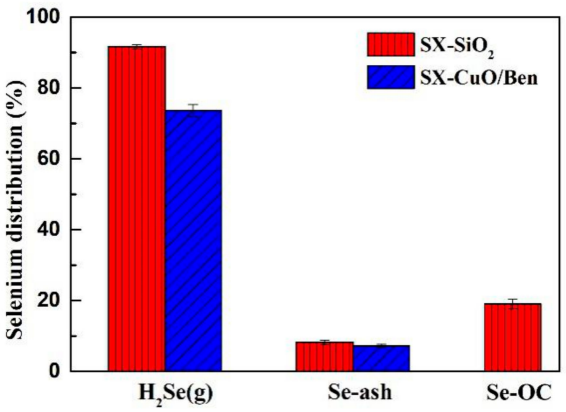

Figure 3. Selenium distribution during coal gasification and CLG.

In order to analyze the existing form of selenium in the OCs, XPS (X-ray photoelectron spectroscopy) characterization was performed on the coal ash and OCs after traditional gasification and CLG. The internal reference for each spectrum was calibrated by the C1s

binding energy (BE) at 284.80 eV. Three peaks at 55.5 eV, 56.5 eV and 57.4 eV could be observed in coal ash sample, as shown in Figure 4a. Based on the NIST X-ray photoelectron spectroscopy database, these three peaks overall represented elemental Se [37]. Because the binding energy of elemental selenium is complex, 55.5 eV, 56.5 eV, 57.4 eV and 54.7 eV represent elemental selenium in Figure 4. However, except for four peaks of elemental selenium, a peak at 53.9 eV was detected in the CuO/Ben OCs after CLG in Figure 4b, which corresponded to the compound Cu_2Se [38]. This indicated that a small amount of selenium migrated to the OC in the form of Cu_2Se during CLG as shown in Table 4.

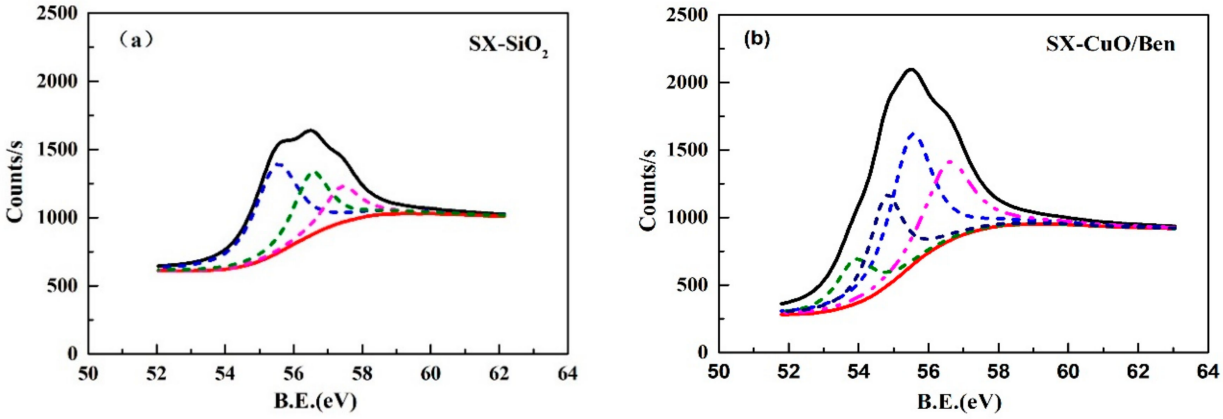

Figure 4. XPS spectra of (**a**) coal ash after conventional gasification and (**b**) reduced CuO/Ben using SX coal after CLG.

Table 4. Percentages of Se species determined from XPS analysis.

Sample	Cu_2Se (%)	Se (%)			
	53.90 eV	55.5 eV	56.5 eV	57.4 eV	54.7 eV
$SX-SiO_2$	-	52.68	29.89	17.43	-
SX-CuO/Ben	12.03	33.57	27.30	-	27.1

3.2.2. Thermodynamic Calculations

Thermal equilibrium calculations can be used to estimate possible reactions and by-products generated. The change in selenium valence is mainly connected with the oxidation capacity of the OCs. Additionally, the reduction products of the OCs with diverse valence states have unequable oxidizing power, which has a significant influence on selenium migration. This important factor should be examined to clarify the influence of reduction products and OCs on the valence conversion of selenium. In this section, the change trend of selenium compounds under the conditions of CLG was analyzed by thermal equilibrium calculation.

$$Se\ (g) + H_2\ (g) = H_2Se\ (g) \quad (R1)$$

$$Se\ (g) + CO(g) + H_2O = H_2Se\ (g) + CO_2\ (g) \quad (R2)$$

$$2\ CuO + H_2Se\ (g) + H_2\ (g) = Cu_2Se + 2\ H_2O \quad (R3)$$

$$H_2Se\ (g) + 2\ Cu = Cu_2Se + H_2\ (g) \quad (R4)$$

$$H_2Se\ (g) + CuO = CuSe + H_2O \quad (R5)$$

$$CuSe + H_2\ (g) + CO\ (g) + 2\ CuO = Cu_2Se + H_2O\ (g) + CO_2\ (g) + Cu \quad (R6)$$

We can see from Figure 5a, that due to the influence of the active component CuO in CLG, H_2Se (g) and Cu_2Se were the two main existing forms of selenium when the temperature range was 100–1000 °C. The differences in the minimum Gibbs criterion of reactions ((R1)–(R6)) with temperature were drawn in Figure 5b. Apparently, H_2Se (g) was regarded

as the primary form of selenium in the gasification atmosphere by reaction (R1) and (R2). At 900 °C, CuO and Cu possessed the power to convert H_2Se (g) to Cu_2Se, as demonstrated by reaction (R3) and (R4). Moreover, CuSe was likely to be generated according to the reaction (R5). After analyzing the reasons for this phenomenon, the explanation was as follows: under a reduced atmosphere, a small number of CuSe would rapidly be converted to Cu_2Se, adhering to the OCs by reaction (R6). Similarly, the verification experiment was carried out in practice. The thermodynamic calculation results were in accordance with the XPS characterization results of the CLG experiments.

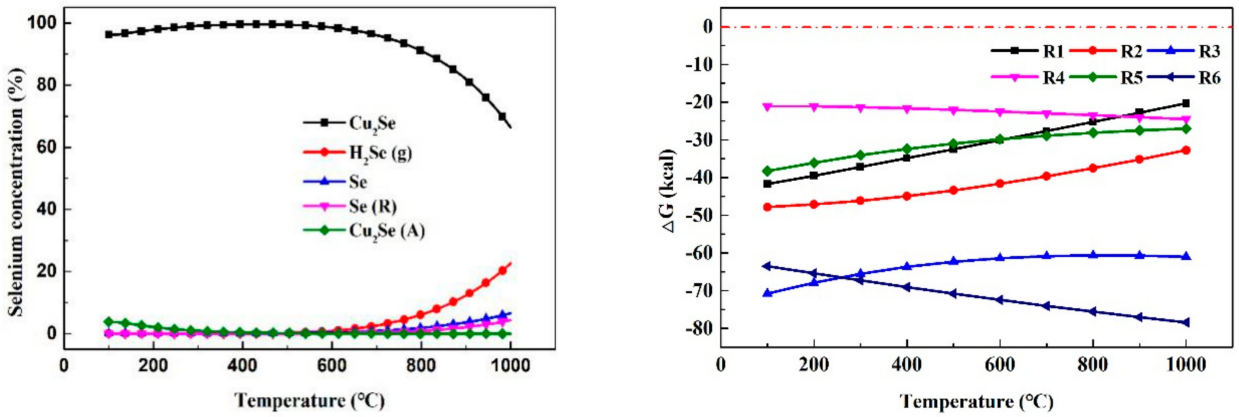

(**a**) (**b**)

Figure 5. (**a**) The existing form of selenium in CLG; (**b**) Gibbs free energy with temperature for reactions ((R1)–(R6)).

3.3. Effects of Experimental Conditions on the Behavior of Selenium

3.3.1. The Effects of Oxygen Carriers

As the key to CLG, OC plays a critical role in influencing the distribution of selenium. The O/C ratio is a significant parameter affecting the CLG process. An O/C ratio that is too high will lead to raw materials being oxidized excessively, while an O/C ratio that is too low cannot achieve a good gasification effect. To explore the impact of the O/C ratio on the migration behavior of selenium, experiments were carried out when the O/C ratio was 0.2, 0.4, 0.6 and 0.8, under identical operation conditions. Figure 6 showed the impact of various O/C ratios on the distribution of selenium.

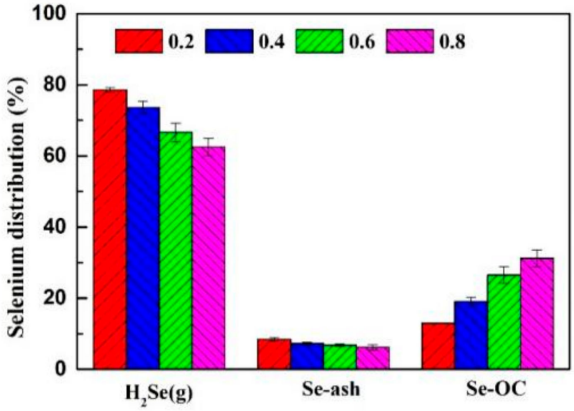

Figure 6. Selenium distribution at different O/C ratio during CLG.

In CLG, with the increase in O/C ratio from 0.2 to 0.8, the proportion of H_2Se (g) in the gas phase decreased from 78.62% to 62.53% and the distribution of selenium in CuO/Ben

OCs increased from 12.96% to 31.26%. The increasing proportion was approximate to the ratio of the increase in OC mass, which indicated that the addition of the O/C ratio was beneficial to the retention of selenium in the OCs. Moreover, the OC mass increased due to the addition of the O/C ratio, which may make the physical adsorption effect of the OCs on selenium obvious.

3.3.2. The Influence of Coal Types

The importance of coal on the migration behavior of selenium cannot be ignored. The selection of coal with a high concentration of selenium in coal is the premise of this study. For the sake of discovering the migration behavior of selenium using different coal types during CLG, we selected Inner Mongolia and Ningxia coal for the same experiment. As shown in Figure 7, in the Inner Mongolia coal and Ningxia coal gasification experiments (with SiO_2 as the bed material), selenium was mostly distributed in the form of gaseous H_2Se (g), accounting for 93.13% and 93.84%, respectively, and the concentration of selenium in coal ash accounted for 6.87% and 6.16%, respectively.

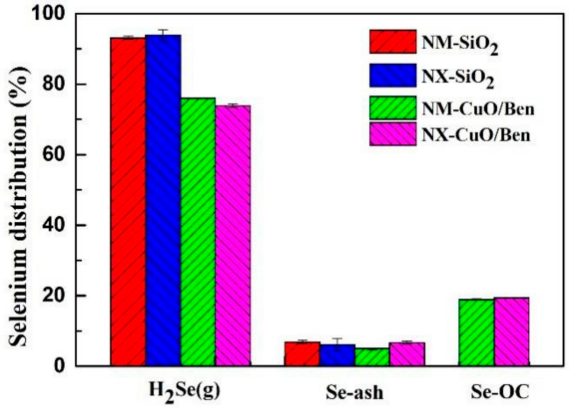

Figure 7. Selenium distribution of NM and MX coal during CLG.

The CLG and conventional gasification process differ because of the influence of lattice oxygen and the active sites, the OCs have the capacity to oxidize and adsorb selenium, and the content of selenium in gaseous H_2Se (g) decreased to 76.07% and 75.90% for the Inner Mongolia and Ningxia coals, respectively, while that in the CuO/Ben OC increased to 18.93% and 18.40%, respectively. The content of selenium in coal ash remained basically unchanged. The above conclusions were consistent with those results obtained by selecting Shaanxi coal as the fuel, which indicated that the laws of selenium migration and transformation during traditional gasification and CLG were universal.

3.3.3. Recycle and Regeneration Performance

The recycling of OC is the guarantee for the industrialization of CLG. The surface structure of CuO/Ben OC facilitates the adsorption of selenium into their porous channels. Hence, it is necessary to understand the recycle regeneration performance of the OC particles. Figure 8 showed the crystal structure changes of CuO/Ben OC in the regeneration process. Through reduction reactions in the gasification reactor, the crystal phase structure of CuO/Ben OC appeared as Cu, and the reduced products were oxidized to CuO in the air atmosphere at 900 °C.

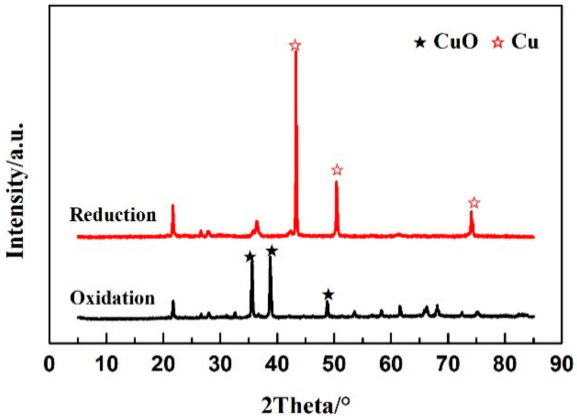

Figure 8. XRD results of reduced and regenerated CuO/Ben oxygen carrier.

Figure 9 shows the crystal structure of CuO/Ben OC in multiple cycle regenerations by XRD (X-ray diffraction) spectra. In the cycle regeneration process at 900 °C, the morphology of OCs remained stable. The distribution of selenium during recycling regeneration of the CuO/Ben OC is shown in Figure 10.

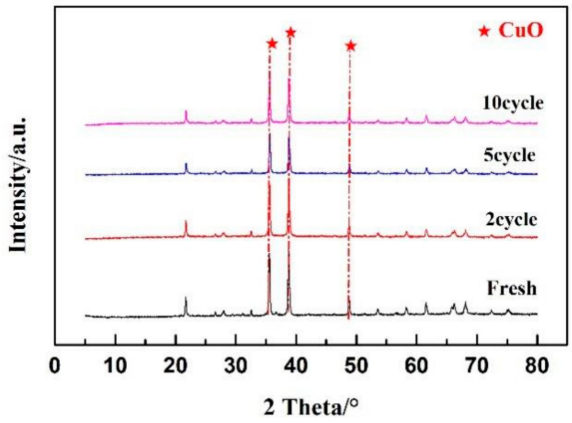

Figure 9. A 10-cycle regeneration test with variations of XRD spectra.

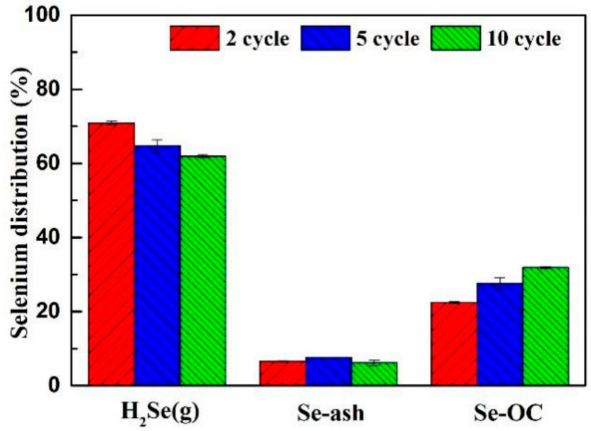

Figure 10. Variations of selenium distribution during a 10-cycle test.

With the recycling period from two cycles to 10 cycles, the release rate of selenium decreased from 70.90% to 61.92%. The distribution of selenium remained basically stable in coal ash, however, the content of selenium in CuO/Ben OCs increased regularly, which demonstrated that the CuO/Ben OC had good recycling performance.

We aimed to thoroughly analyze the reasons why selenium was retained by the CuO/Ben OCs in CLG. As shown in Table 5 and Figure 11, some characterizations of SEM (Scanning electron microscopy), EDS, pore volumes and specific surface area analysis were conducted on the regenerated CuO/Ben OCs. Fresh CuO/Ben OC has more pores and a denser pore distribution.

Table 5. The material texture of fresh and 10-cycle CuO/Ben oxygen carrier.

Sample	S_{BET} (m^2/g)	Pore Volume (cm^3/g)
Fresh	0.578	0.121
2 Cycles	0.668	0.130
5 Cycles	1.233	0.143
10 Cycles	1.809	0.168

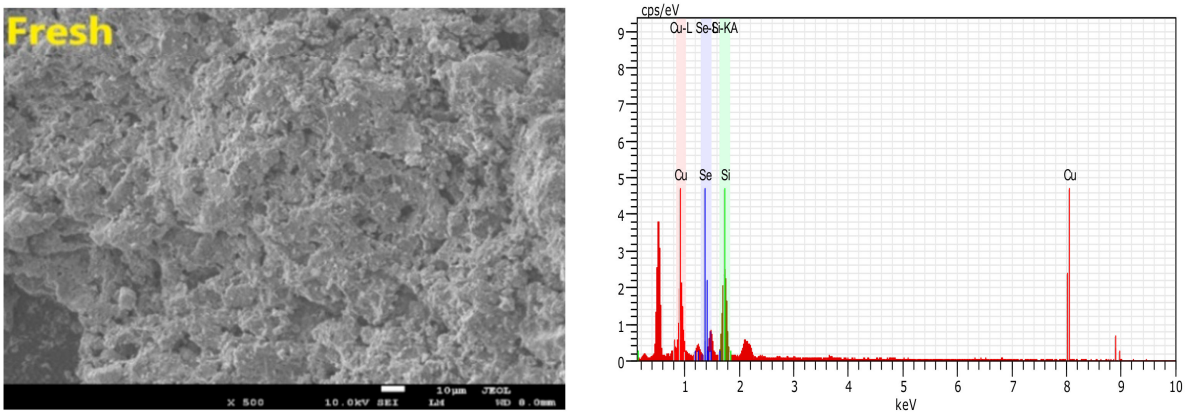

(**a**)

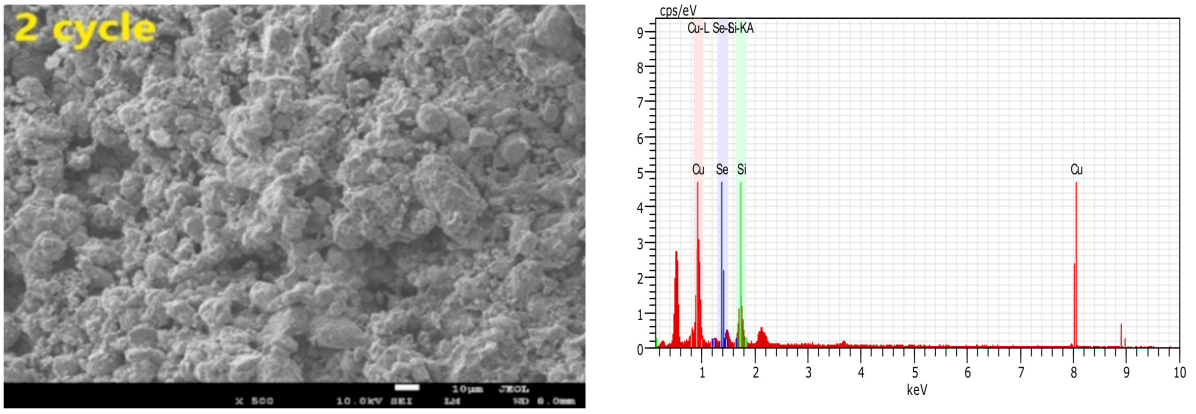

(**b**)

Figure 11. *Cont.*

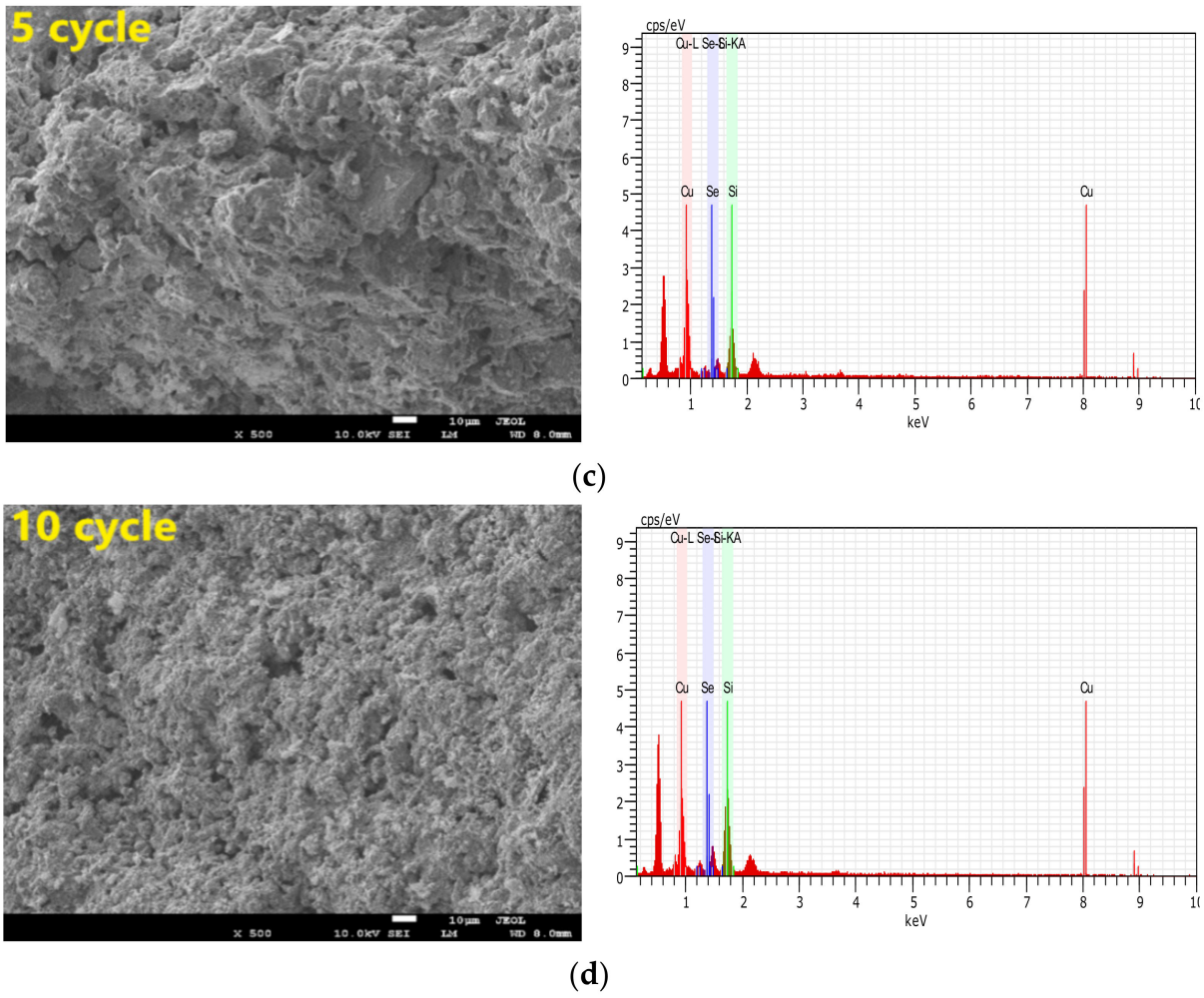

Figure 11. SEM and EDS images of SX bitumite samples with CuO/Ben oxygen carrier: (**a**) Fresh samples; (**b**) after two cycles; (**c**) five cycles and (**d**) 10 cycles.

With the increase in the regeneration cycle, the porous channels of the CuO/Ben OC were enhanced, and there existed no sintering phenomenon at the same time, indicating that the OC has good cycle stability, as shown in Figure 11. In Figure 11 we can find that the retention of selenium by OC is relatively stable as the number of cycles increases. The retention effect of selenium by OC did not change as cycles increased. Selenium can still be detected in the 10th cyclic experiment as shown in Figure 11d. The data in Table 5 confirmed the SEM and EDS observation results. The specific surface area of fresh particles was 0.578 m^2/g, and while five cycles were completed, the specific surface areas of CuO/Ben OC added up to 1.233 m^2/g, with pore volumes increasing from 0.121 cm^3/g to 0.143 cm^3/g. Until the regeneration cycle was executed 10 times, the specific surface area of CuO/Ben OC further increased to 1.809 m^2/g, and the pore volume increased to 0.168 cm^3/g. Hence, with the increase in regeneration cycles, the capacity of CuO/Ben OCs to retain selenium was strengthened due to the increased surface pore structure.

4. Conclusions

The action mechanism of coal and metal oxides can be divided into the following aspects. The gaseous H_2Se (g) was mainly generated as the coal reacted with the products during coal gasification at 900 °C. However, in the CLG process, H_2Se (g) interacted with CuO, Cu and the products generated in the process of coal pyrolysis and gasification, to produce Cu_2Se and Se, and attached to the surface of the OCs. In addition, selenium in coal

ash and most OCs existed in the form of elemental selenium. The specific conclusions are stated below:

1. During the CLG process, the distribution of selenium in the flue gas, coal ash and OCs is 73.65%, 7.28% and 19.07%, respectively. The CuO/Ben oxygen carrier promoted the transformation of the gaseous selenium to particulate selenium.
2. As the oxygen–carbon ratio increased from 0.2 to 0.8, the content of H_2Se (g) decreased from 78.62% to 62.53%, and the content of selenium in the oxygen carrier increased from 12.96% to 31.26%, indicating that the oxygen–carbon ratio increase improved the conversion ability of H_2Se (g) to Cu_2Se. The behavior of selenium during CLG is generally suitable to SX, NX, NM coals.
3. By acquisition of lattice oxygen and the thermal decomposition of selenium, the reduced CuO/Ben OCs were regenerated in an air reactor. With the regeneration cycles increased to 10 times, the capacity of the CuO/Ben OCs to capture selenium was strengthened slightly.

Author Contributions: Conceptualization, J.M. and Q.G.; Data curation, J.M., J.H. and Q.G.; Investigation, J.M., J.H. and Z.H.; Methodology, H.K. and Z.H.; Resources, H.K.; Writing—original draft, J.M. and J.H.; Writing—review & editing, J.M. All authors have read and agreed to the published version of the manuscript.

Funding: This work is funded by the National Natural Science Foundation of China (201868025); the Key Research and Development Program Project of Ningxia (2018BEE03009); and the National First-rate Discipline Construction Project of Ningxia (NXYLXK2017A04).

Institutional Review Board Statement: Not applicable.

Informed Consent Statement: Not applicable.

Data Availability Statement: Not applicable.

Conflicts of Interest: The authors declare no competing financial interest.

References

1. Guo, Q.J.; Chen, Y.; Liu, Y.Z.; Jia, W.H.; Ryu, H.J. Coal chemical looping gasification for syngas generation using an iron-based oxygen carrier. *Ind. Eng. Chem. Res.* **2013**, *53*, 78–86. [CrossRef]
2. Guo, Q.J.; Hu, X.D.; Liu, Y.Z.; Jia, W.H.; Yang, M.M.; Wu, M.; Tian, H.J.; Ryu, H.J. Coal chemical-looping gasification of Ca-based oxygen carriers decorated by CaO. *Powder Technol.* **2015**, *275*, 60–68. [CrossRef]
3. Duan, W.; Yu, Q.B. Thermodynamic analysis of hydrogen-enriched syngas generation coupled with in situ CO_2 capture using chemical looping gasification method. *J. Therm. Anal. Calorim.* **2018**, *131*, 1671–1680. [CrossRef]
4. Liu, Y.Z.; Jia, W.H.; Guo, Q.J.; Ryu, H.J. Effect of gasifying medium on the coal chemical looping gasification with $CaSO_4$ as oxygen carrier. *Chin. J. Chem. Eng.* **2014**, *22*, 1208–1214. [CrossRef]
5. Wang, P.; Means, N.; Shekhawat, D.; Berry, D.; Massoudi, M. Chemical-looping combustion and gasification of coals and oxygen carrier development: A brief review. *Energies* **2015**, *8*, 10605–10635. [CrossRef]
6. Pishahang, M.; Larring, Y.; Adánez, J.; Gayán, P.; Sunding, M. Fe_2O_3-Al_2O_3 oxygen carrier materials for chemical looping combustion, a redox thermodynamic and thermogravimetric evaluation in the presence of H_2S. *J. Therm. Anal. Calorim.* **2018**, *134*, 1739–1748. [CrossRef]
7. Wang, Y.D.; Wang, X.Y.; Hua, X.N.; Zhao, C.C.; Wang, W. The reduction mechanism and kinetics of Fe_2O_3 by hydrogen for chemical-looping hydrogen generation. *J. Therm. Anal. Calorim.* **2017**, *129*, 1831–1838. [CrossRef]
8. Song, G.C.; Xu, W.T.; Liu, K.; Song, Q. Transformation of selenium during coal thermal conversion: Effects of atmosphere and inorganic content. *Fuel Process. Technol.* **2020**, *205*, 106446. [CrossRef]
9. Fraga, C.G. Relevance, essentiality and toxicity of trace elements in human health. *Mol. Asp. Med.* **2005**, *26*, 235–244. [CrossRef] [PubMed]
10. Winkel, L.H.E.; Johnson, C.A.; Lenz, M.; Grundl, T.; Leupin, O.X.; Amini, M.; Charlet, L. Environmental selenium research: From microscopic processes to global understanding. *Environ. Sci. Technol.* **2011**, *46*, 571–579. [CrossRef]
11. Chen, G.Y.; Sun, Y.N.; Yan, B.B.; Yang, R.L.; Liu, B.; Cheng, Z.J.; Ma, W.C. Distribution of trace elements during coal gasification: The effect of upgrading method. *J. Clean. Prod.* **2018**, *190*, 193–199. [CrossRef]
12. Hussain, R.; Luo, K.L. Geochemical valuation and intake of F, As, and Se in coal wastes contaminated areas and their potential impacts on local inhabitants, Shaanxi China. *Environ. Geochem. Health* **2018**, *40*, 2667–2683. [CrossRef] [PubMed]

13. López-Antón, M.A.; Díaz-Somoano, M.; Fierro, J.L.G.; Martínez-Tarazona, M.R. Retention of arsenic and selenium compounds present in coal combustion and gasification flue gases using activated carbons. *Fuel. Process. Technol.* **2007**, *88*, 799–805. [CrossRef]
14. Yuan, C.L.; Zhang, C.; Yu, S.H.; Xu, H.; Li, X.; Fang, Q.; Chen, G. Experimental and density functional theory study of the adsorption characteristics of CaO for SeO_2 in simulated flue gas and the effect of CO_2. *Energy Fuels* **2020**, *34*, 10872–10881. [CrossRef]
15. Diaz-Somoano, M.; Martinez-Tarazona, M.R. Retention of arsenic and selenium compounds using limestone in a coal gasification flue gas. *Environ. Sci. Technol.* **2004**, *38*, 899–903. [CrossRef]
16. Furuzono, T.; Nakajima, T.; Fujishima, H.; Takanashi, H.; Akira, O. Behavior of selenium in the flue gas of pulverized coal combustion system: Influence of kind of coal and combustion conditions. *Fuel Process. Technol.* **2017**, *167*, 388–394. [CrossRef]
17. Yan, R.; Gauthier, D.; Flamant, G.; Peraudeau, G.; Lu, J.D.; Zheng, C.G. Fate of selenium in coal combustion: Volatilization and speciation in the flue gas. *Environ. Sci. Technol.* **2001**, *35*, 1406–1410. [CrossRef]
18. Shen, F.H.; Liu, J.; Zhang, Z.; Yang, Y.J. Temporal measurements and kinetics of selenium release during coal combustion and gasification in a fluidized bed. *J. Hazard. Mater.* **2016**, *310*, 40–47. [CrossRef]
19. Fu, B.; Hower, J.C.; Dai, S.F.; Mardon, S.M.; Liu, G.J. Determination of chemical speciation of arsenic and selenium in high-As coal combustion ash by X-ray photoelectron spectroscopy: Examples from a Kentucky stoker ash. *ACS Omega* **2018**, *3*, 17637–17645. [CrossRef]
20. Mendiara, T.; Izquier, M.T.; Abad, A.; Gayan, P.; Garcia-Labiano, F.; de Diego, L.F.; Adanez, J. Mercury release and speciation in chemical looping combustion of coal. *Energy Fuels* **2014**, *28*, 2786–2794. [CrossRef]
21. An, M.; Ma, J.J.; Guo, Q.J. Transformation and migration of mercury during chemical-Looping gasification of coal. *Ind. Eng. Chem. Res.* **2019**, *58*, 20481–20490. [CrossRef]
22. Li, W.H.; Song, N.; Zhang, Y.S.; Cao, Y.; Orndorff, W.; Pan, W.P. Mercury sorption properties of HBr-modified fly ash in a fixed bed reactor. *J. Therm. Anal. Calorim.* **2016**, *124*, 387–393. [CrossRef]
23. Yan, R.; Gauthier, D.; Flamant, G.; Wang, Y.M. Behavior of selenium in the combustion of coal or coke spiked with Se. *Combust. Flame* **2004**, *138*, 20–29. [CrossRef]
24. Wang, J.W.; Zhang, Y.S.; Wang, T.; Xu, H.; Pan, W.P. Effect of modified fly ash injection on As, Se, and Pb emissions in coal-fired power plant. *Chem. Eng. J.* **2020**, *380*, 122561. [CrossRef]
25. Chen, P.; Sun, X.Q.; Gao, M.G.; Ma, J.J.; Guo, Q.J. Transformation and migration of cadmium during chemical-looping combustion/gasification of municipal solid waste. *Chem. Eng. J.* **2019**, *365*, 389–399. [CrossRef]
26. Ma, J.C.; Mei, D.F.; Tian, X.; Zhang, S.B.; Yang, J.P.; Wang, C.Q.; Chen, G.P.; Zhao, Y.C.; Zheng, C.G.; Zhao, H.B. Fate of mercury in volatiles and char during in situ gasification chemical-looping combustion of coal. *Environ. Sci. Technol.* **2019**, *53*, 7887–7892. [CrossRef]
27. Ma, J.C.; Wang, C.Q.; Zhao, H.B.; Tian, X. Sulfur fate during the lignite pyrolysis process in a chemical looping combustion environment. *Energy Fuels* **2018**, *32*, 4493–4501. [CrossRef]
28. Sui, Z.F.; Zhang, Y.S.; Li, W.H.; Orndorff, W.; Cao, Y.; Pan, W.P. Partitioning effect of mercury content and speciation in gypsum slurry as a function of time. *J. Therm. Anal. Calorim.* **2015**, *119*, 1611–1618. [CrossRef]
29. Niu, X.; Shen, L.H. Release and transformation of phosphorus in chemical looping combustion of sewage sludge. *Chem. Eng. J.* **2018**, *335*, 621–630. [CrossRef]
30. Nasah, J.; Jensen, B.; Dyrstad-Cincotta, N.; Gerber, J.; Laudal, D.; Mann, M.; Srinivasachar, S. Method for separation of coal conversion products from oxygen carriers. *Int. J. Greenh. Gas Control.* **2019**, *88*, 361–370. [CrossRef]
31. Monazam, E.R.; Breault, Q.W.; Siriwardane, R.; Tian, H.J.; Simonyi, T.; Carpenter, S. Effect of carbon deposition on the oxidation rate of copper/bentonite in the chemical looping process. *Energy Fuels* **2012**, *26*, 6576–6583. [CrossRef]
32. Darwish, E.; Yılmaz, D.; Leion, H. Experimental and thermodynamic study on the interaction of copper oxygen carriers and oxide compounds commonly present in ashes. *Energy Fuels* **2019**, *33*, 2502–2515. [CrossRef]
33. Sun, J.; Yang, Y.D.; Liu, W.Q. Evaluating redox reactivity of CuO-based oxygen carriers synthesized with organometallic precursors. *J. Therm. Anal. Calorim.* **2020**, *139*, 885–893. [CrossRef]
34. Wang, X.; Xu, T.T.; Jin, X.Y.; Hu, Z.Q.; Liu, S.M.; Xiao, B.; Chen, Z.H.; Hu, M. CuO supported on olivine as an oxygen carrier in chemical looping processes with pine sawdust used as fuel. *Chem. Eng. J.* **2017**, *330*, 480–490. [CrossRef]
35. Guo, Q.J.; Liu, Y.Z.; Jia, W.H.; Yang, M.M.; Hu, X.D.; Ryu, H.J. Performance of Ca-Based oxygen carriers decorated by K_2CO_3 or Fe_2O_3 for coal chemical looping combustion. *Energy Fuels* **2014**, *28*, 7053–7060. [CrossRef]
36. *ISO 17211:2015*; Stationary Source Emissions—Sampling and Determination of Selenium Compounds in Flue Gas. International Organization for Standardization: Geneva, Switzerland, 2015.
37. Alexander, V.N.; Anna, K.V.; Stephen, W.G.; Cedric, J. *Distributed by the Measurement Services Division of the National Institute of Standards and Technology (NIST) Material Measurement Laboratory (MML)*; Material Measurement Laboratory: Gaithersburg, MD, USA, 2012.
38. Wu, L.T.; Chen, H.; Zhang, K.Y.; Qin, A.M.; Chen, S.P. Room-temperature rapid synthesis of Cu_2Se_x and its phase transformation to CuO by electrochemical method. *J. Alloy. Compd.* **2019**, *797*, 497–503. [CrossRef]